Arabian Sea upwelling – A comparison between coastal and open ocean regions

P. M. Muraleedharan and S. Prasanna Kumar

National Institute of Oceanography, Dona Paula, Goa 403 004, India

The response of the eastern Arabian Sea to prevailing winds during an upwelling event, in the peak of southwest monsoon, was studied at both coastal and open ocean environment based on the data collected as a part of the Indian Joint Global Ocean Flux Studies (JGOFS) programme. Analysis of wind measurements indicated active upwelling along the southwest coast of India, which gradually propagates towards north. While the dominant long-shore component of the wind induces upwelling in the south, the cross-shore component is instrumental in modifying the density structure of the surface layer, especially in the north, to produce retarding effect. In open ocean, the wind maximum around 17° N and 64° E indicates the axis of the Findlater Jet. The observed surfacing and deepening of the isotherms on either side of the axis are the signatures of the upwelling and sinking associated with the Findlater Jet.

CLASSICAL explanation of coastal upwelling favours wind-induced divergence caused by Ekman transport of the surface water away from the coast[1]. The concept is widely supported by observations[2,3] as well as by theoretical models[4–7]. Although comprehensive literature on the coastal upwelling system in the Arabian Sea exists, information on open ocean upwelling is somehow scanty. Bauer *et al.*[8] observed seasonal occurrence of wind-induced upwelling in the northern Arabian Sea, wherein considerable shoaling of the thermocline occurred under the region of maximum winds (Findlater Jet).

In the present paper we examine both coastal and open ocean upwelling during southwest monsoon season. To this end a cruise was undertaken during the peak of the southwest monsoon season (July–August 1995).

Data and methodology

The present investigation is based on the data collected onboard ORV *Sagar Kanya* from 20th July to 12th August 1995, as a part of the Indian Joint Global Ocean Flux Studies (JGOFS) Programme. A Sea Bird CTD was used to collect temperature–salinity profiles from 42 stations up to a maximum depth of 1000 m (Figure 1). Surface meteorological data were collected at six hourly interval along the track. Climatological wind and sea surface temperature (SST) derived from Comprehensive Oceanographic and Atmospheric Data Set (COADS)[9] and mixed layer depth (MLD) from Levitus data[10] were also used for comparison with the *in situ* measurements.

Results and discussion

Wind field

The climatological wind during July indicates strong cross-shore component with positive trends from south to north and relatively weak long-shore component with similar trend, except at 15°N where a steep rise in wind speed is noticed (Figure 2 *a*). The SST and MLD distributions also followed the same trend as the wind. It is hence inferred that an upwelling favourable condition existed along the southern shelf, which was less conspicuous towards north.

In the central Arabian Sea, along 64° E, both the zonal

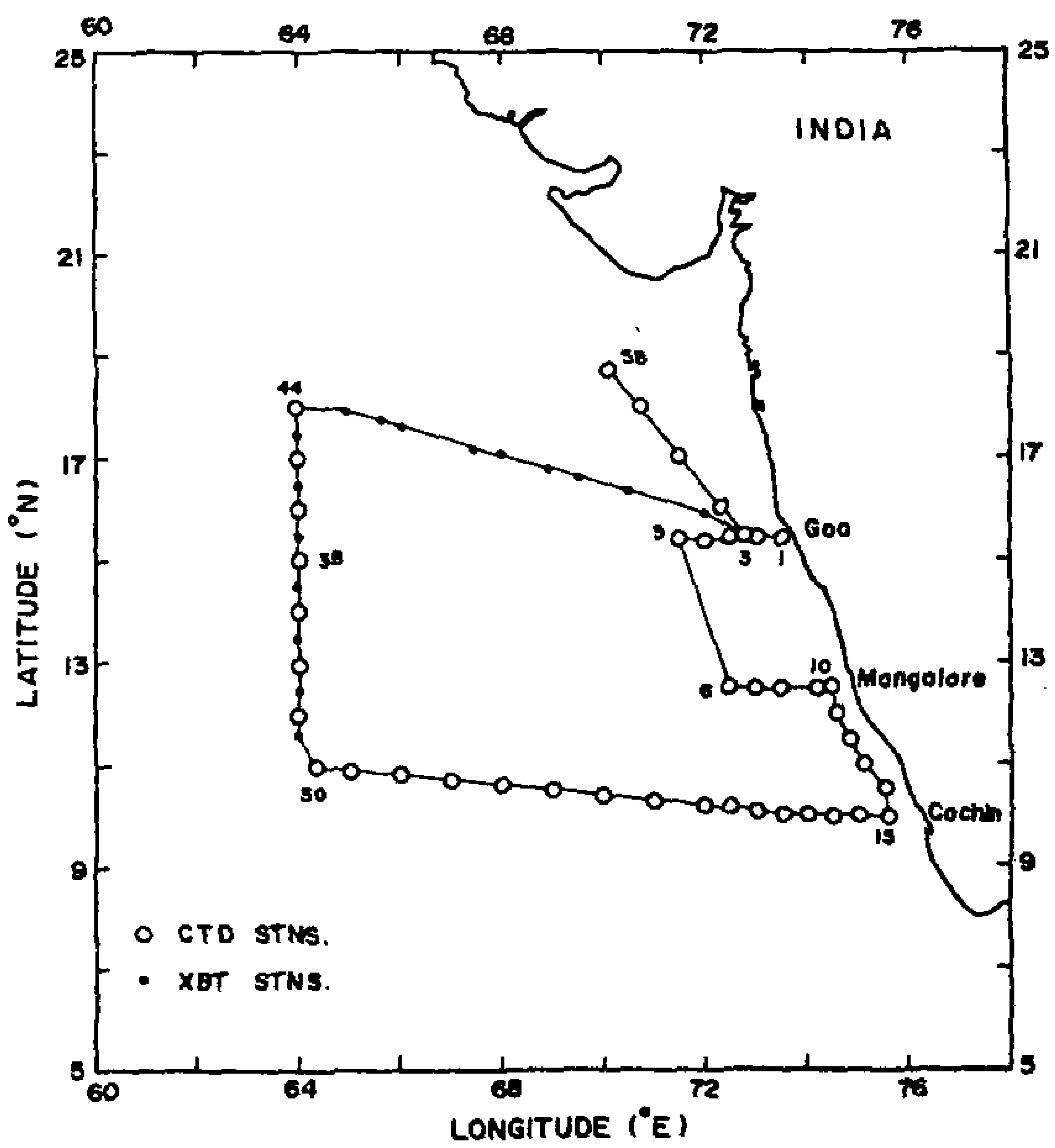

Figure 1. Cruise track and station locations.

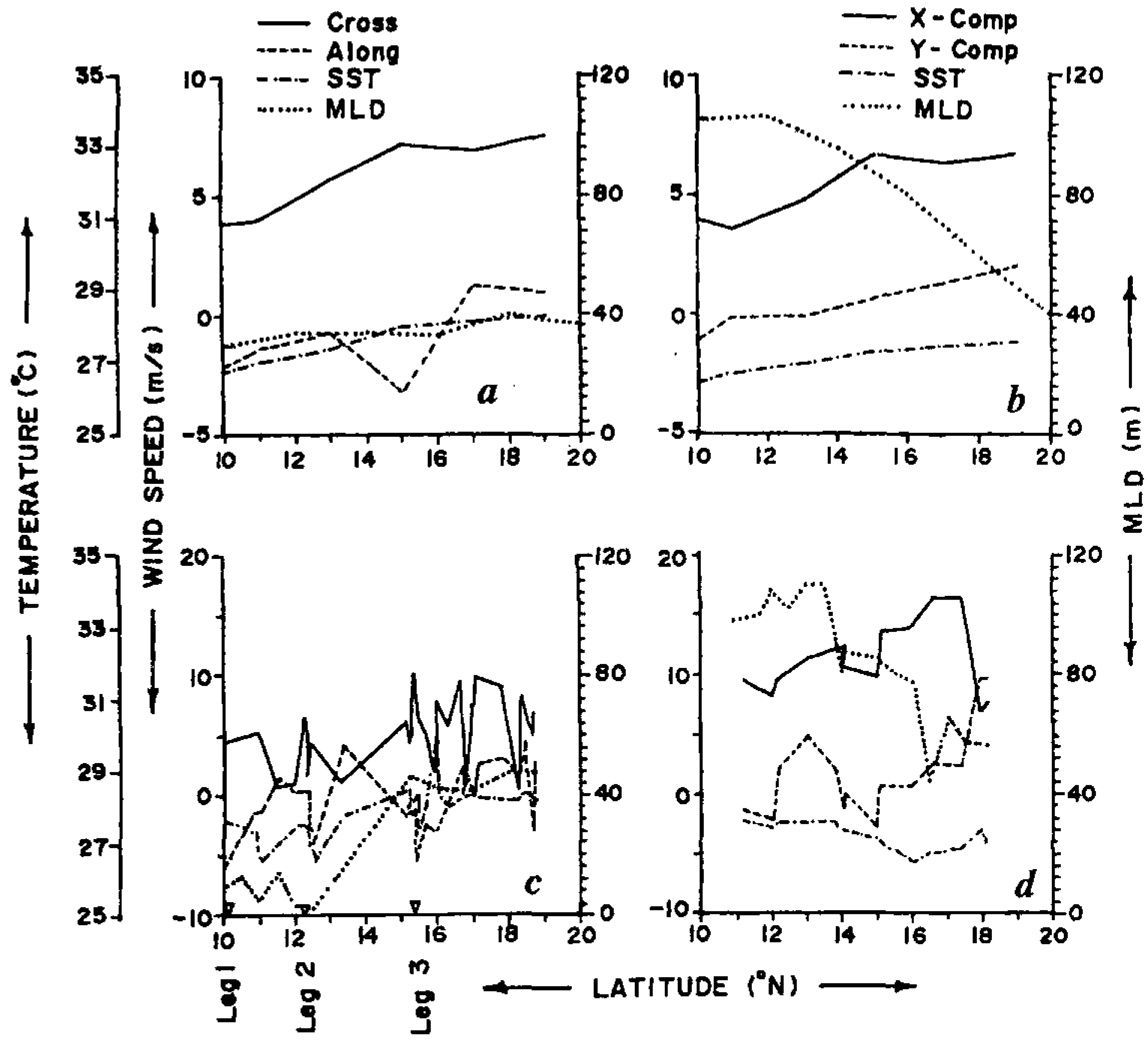

Figure 2 ***a–d*****.** Variation of zonal and meridional wind component, sea surface temperature (SST) and mixed layer depth (MLD) from 10°N to 20°N along the west coast of India [climatological (*a*) and insitu (*c*)] and along 64° E [climatological (*b*) and *in situ* (*d*)] are plotted against latitude during July.

and the meridional components of the wind showed gradual increase from south to north (Figure 2 *b*). The zonal component was maximum around 17°N and decreased towards north. SST showed a gradual increase of 1°C from south to north. A thick MLD of 110 m was noticed at 10° N, which dropped to 40 m around 20° N. The high zonal component of the wind around 17° N represents the axis of the Findlater Jet. However, the climatological SST distribution does not imply an upwelling at the region of wind maximum.

In order to decipher the upwelling along the coast, *in situ* data were collected at three legs (Figure 1), viz. off Goa (15°N), off Mangalore (12.5°N) and off Cochin (10°N). The observed wind showed a steep rise in both cross-shore (positive towards east) and along-shore (negative towards south) components in all the three legs (Figure 2 *c*). High eastward wind component (10 ms^{-1}) was observed at leg 1 associated with moderately strong southward component (6 ms^{-1}). At leg 2 (off Mangalore) both eastward and southward components had the same magnitude of 4 ms^{-1}. However at leg 3 (off Cochin) the negative long-shore component (northerly wind) dominates over the positive cross-shore component (westerly wind), ➲

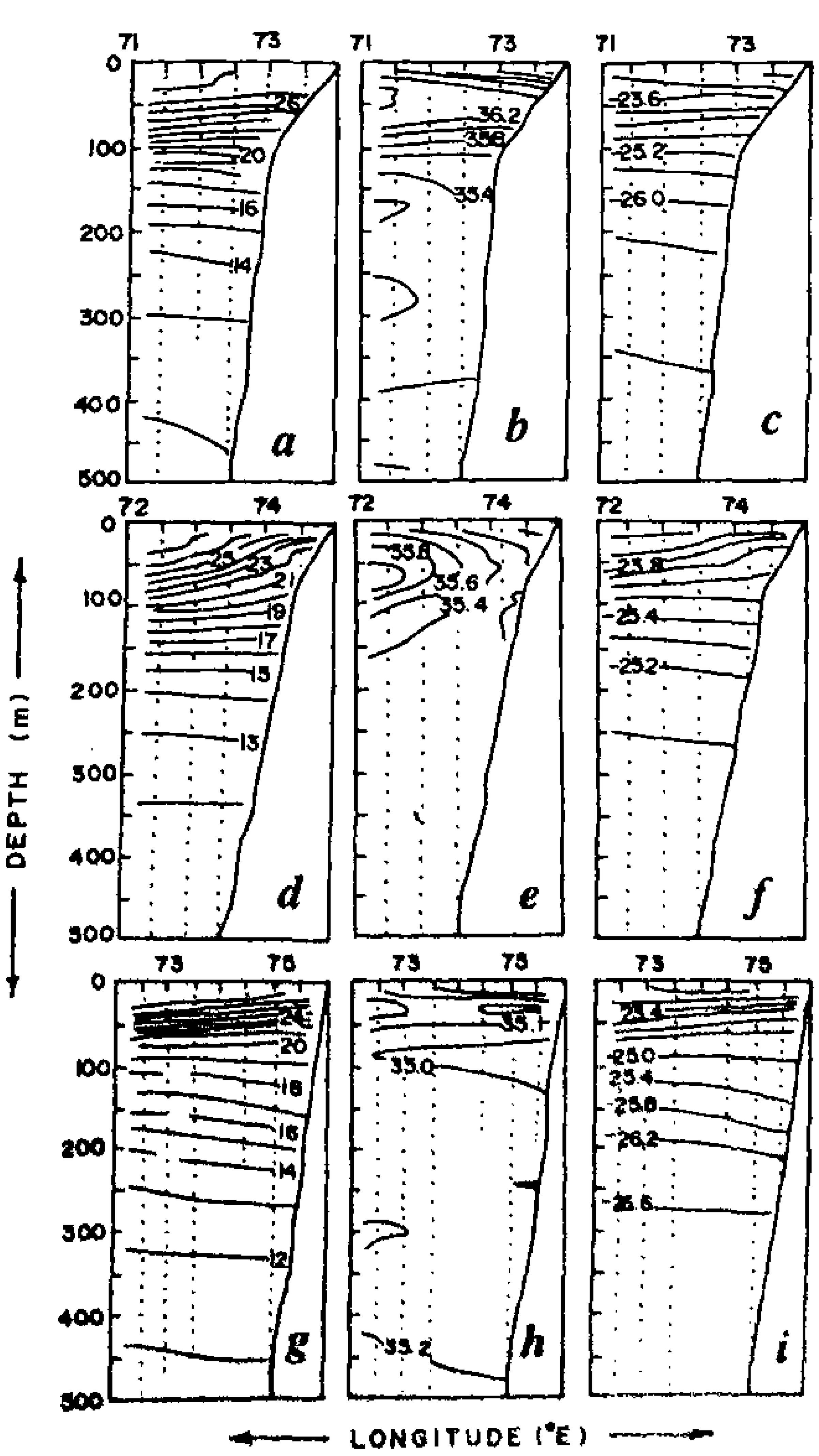

Figure 3 ***a–i*****.** Vertical distribution of temperature (*a, d, g*), salinity (*b, e, h*) and density (*c, f, i*) along legs 1 (off Goa, top panel), 2 (off Mangalore, middle panel) and 3 (off Cochin, bottom panel).

with their magnitudes exceeding 6 and 4 ms^{-1}, respectively (Figure 2 *c*). The shoaling of the isotherm with low SST off Cochin and Mangalore indicated strong upwelling, and were well correlated with the prevailing wind (Figure 2 *c*). Off Goa, though the along-shore wind component and the relatively low SST indicated divergence, the high value of MLD does not support the presence of an active upwelling. This is due to strong cross-shore wind present at this latitude, bringing the saline surface water towards the coast which modifies the density field to supress upwelling. Thus it is obvious that both long-shore as well as cross-shore components play significant role in the dynamics of the underlying water column.

The observed wind and SST along 64°E differ considerably from the climatology, whereas the MLD distribution was consistent. Strong zonal wind component was noticed from 15°N to 18°N with weak meridional component (Figure 2 *d*). The wind maxima at 17°N (Findlater Jet) coincides with the lowest MLD value of 45 m. The remarkable shoaling of MLD from 100 m at 11°N to 45 m at 17°N was associated with active upwelling and sinking on either side of the wind maximum. This is consistent with the SST distribution where cool water is found at the zone of maximum wind and warm water southward.

Hydrographic field

The vertical thermal structure off Goa (Figure 3 *a*) exhibits gentle upsloping of isotherms towards the coast producing colder surface water. However, this trend is reversed in the sub-thermocline region and the isotherms were deepening towards the coast. Surface salinities near the coast were almost 0.8 PSU lower than the offshore values (Figure 3 *b*). Below 200 m, however, there were no appreciable changes in the salinity. The down sloping of the isopycnals towards the coast indicated the dominance of salinity over temperature in the density field (Figure 3 *c*). This disappears in the sub-thermocline region where the distribution of density becomes analogous to that of temperature. The isopycnals at the sub-thermocline depth also followed the same

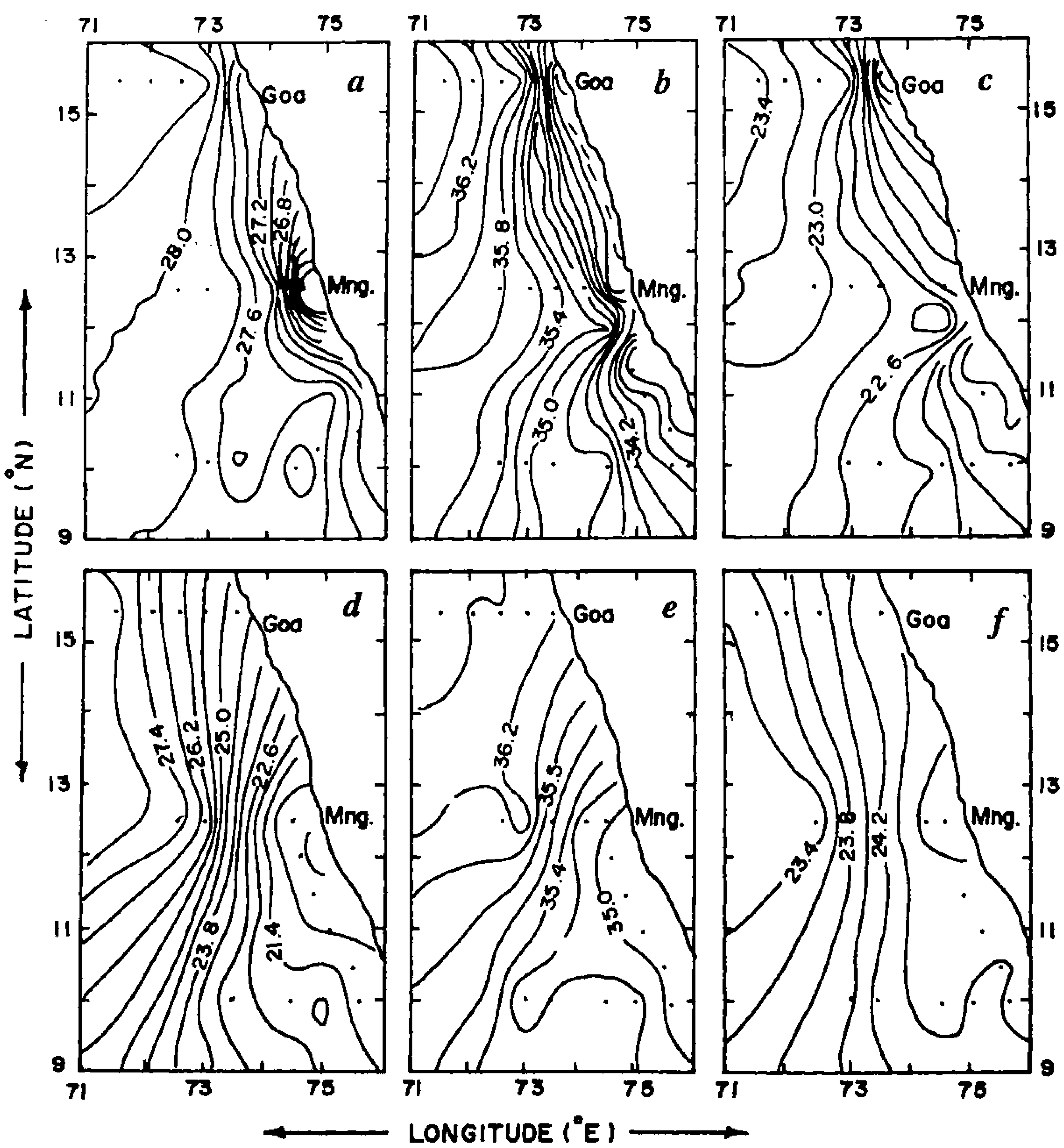

Figure 4 *a–f*. Horizontal distribution of temperature (*a*), salinity (*b*), and density (*c*) at the surface and at 50 m (*d, e, f*) respectively. Note the change in the contour interval of temperature at 50 m.

trend as the temperature. This feature was more conspicuous at the 200 m depth.

The nearshore values of SST off Mangalore were much lower (<23°C) when compared to the offshore values (>27°C) with a gradient of 0.01°C per km (Figure 3 *d*). The remarkable shoaling of thermocline towards the coast is an indication of the active upwelling which is again reflected in the density distribution (Figure 3 *f*). Salinity near the coast was as low as 35 PSU (Figure 3 *e*). Deepening of isotherms and isopynals at the sub-thermocline depth is noticed at this latitude also.

Although the SST off Cochin did not show any appreciable change, the subsurface isotherms above 100 m did indicate gentle upward sloping towards the coast (Figure 3 *g*). The deepening of isotherms and isopycnals in the sub-thermocline region is more pronounced at this latitude (Figure 3 *g* & *i*). The salinity section, in general, does not have any commendable features (Figure 3 *h*).

The strong thermal front identified off Mangalore, from the horizontal temperature field, is the manifestation of an active upwelling system (Figure 4 *a*). Similar features were not observed off Goa and Cochin. The high salinity tongue near Goa and Mangalore was an indication of on-shore transport of surface water as a result of the prevailing winds (Figure 4 *b*). The surface density distribution showed the occurrence of lighter water along the shelf and denser water off-shore (Figure 4 *c*). The thermal gradient at 50 m was three times higher than the surface value with gradient greater than 0.03°C per km (Figure 4 *d*). The intrusion of high salinity water from the central Arabian Sea, as observed at the surface, was less conspicuous at this depth (Figure 4 *e*). The lateral density distribution reversed with denser water along the coast and lighter water offshore (Figure 4 *f*). The temperature field at 100 m depth is dominated by eddy-like circulation (Figure 5 *a*). Penetration of high salinity water from north was seen as a well-developed tongue at this depth (Figure 5 *b*). There was not much lateral variation in density (Figure 5 *c*). At 200 m, the thermohaline structure was entirely different from that at 100 m (Figure 5 *d* and *e*). However, a re-

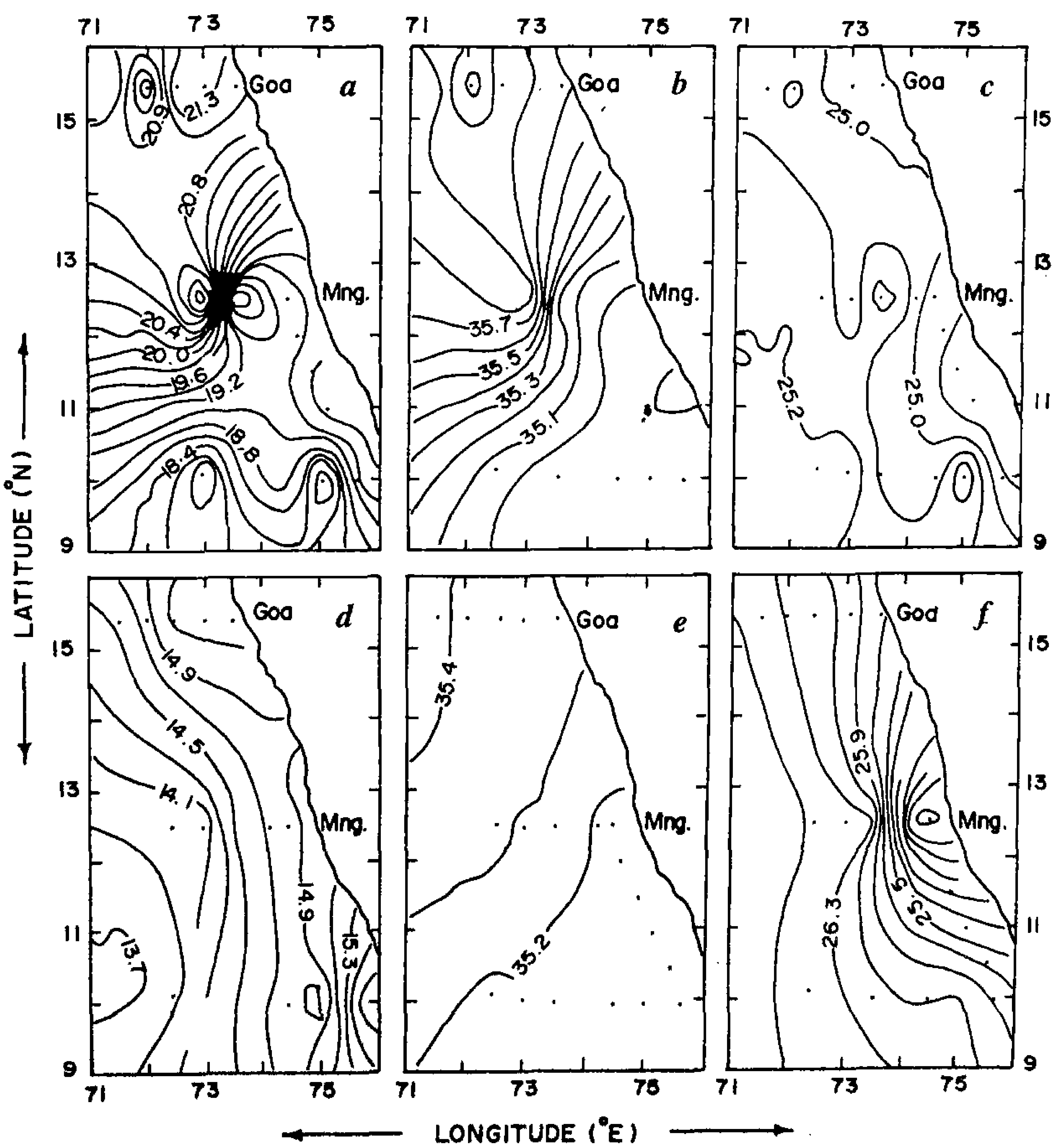

Figure 5 *a–f*. Horizontal distribution of temperature (*a*), salinity (*b*), and density (*c*) at 100 m and at 200 m (*d*, *e*, *f*, respectively).

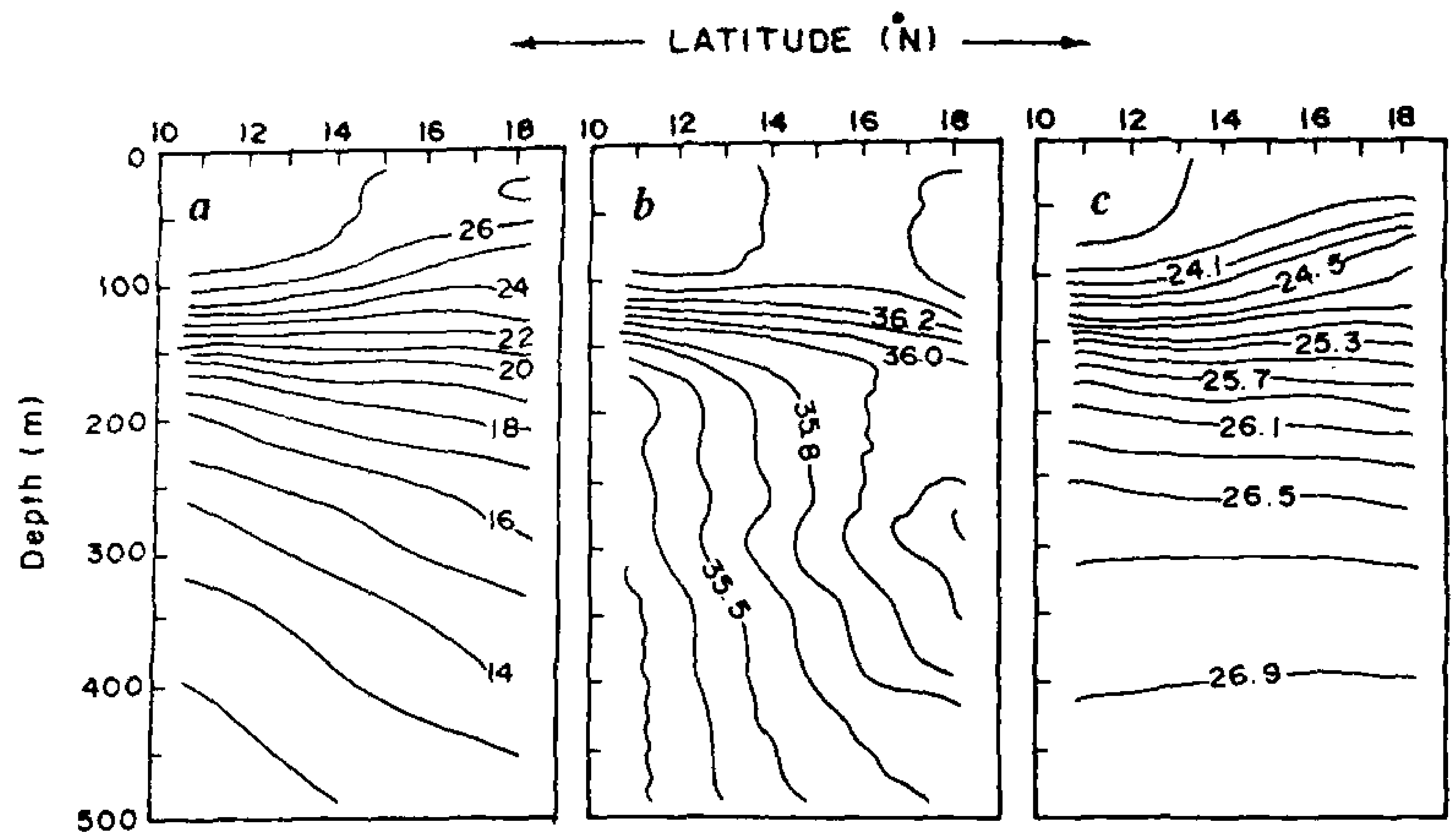

Figure 6. Vertical distribution of temperature (*a*), salinity (*b*), and density (*c*) along 64° E.

versal of lateral density distribution was observed again at this depth with relatively stronger gradient near Mangalore (Figure 5*f*).

Along 64°E, the shoaling of the isotherms above 150 m was a direct indication of open ocean upwelling north of 14°N (Figure 6 *a*), while the deep MLD (110 m) towards south was associated with sinking. The high salinity core observed at 300 m around 18°N was the Persian Gulf water (PGW) mass, which spreads southward. Below 200 m, both temperature as well as salinity structure showed sinking, resulting in a vertically homogeneous salinity structure (Figure 6 *b*). However, the density structure was analogous to that of temperature in the upper 150 m layer. In the sub-thermocline depth, density structure differed from that of temperature due to the proximity of PGW.

In summary, the wind field along the south west coast of India favoured strong upwelling off Cochin, less strong off Mangalore and relatively weak off Goa. Hydrography also supported this, except off Cochin where data close to the coast were not adequate to make the comparison. The stronger subsurface upwelling front (thermal) in comparison to the surface (the gradient of which was three times the surface value) indicates that the regional dynamics suppresses the surface divergence. A plausible explanation could be sought from the prevailing wind forcing. The cross-shore component of the wind pushes the surface high salinity water (ASHSW) towards the coast which modifies the density field along the shelf and suppresses the Ekman pumping mechanism. In the sub-thermocline depth (200 m) the density distribution indicated the presence of a coastal undercurrent which is consistent with the earlier studies[11,12]. The eddy-dominated circulation seen at the bottom of the thermocline (100 m) is the manifestation of frontal instability at the interface between the surface coastal current and the subsurface undercurrent. The open ocean upwelling occurs under the influence of the Findlater Jet, the axis of which was located at 17°N, towards the north while sinking to the south.

1. Sverdrup, H. U., *J. Mar. Res.*, 1938, **V. I**, 155–164.
2. Weaks, M. L., *Oceanogr. Mon. Summ.*, 1983, **3**, 13.
3. Alvarez Salgado, X. L., Roson, G., Perez, P. F. and Pazos, Y., *J. Geophy. Res.*, 1993, **98**, 14447–14455.
4. Yoshida, K., *Jap. J. Geophys.*, 1967, **4**, 1–75.
5. Mc Creary, J. P., *Philos. Trans. R. Soc. London*, 1981, **302**, 385–413.
6. Suginohara, N., *J. Phys. Oceanogr.*, 1982, **12**, 272–284.
7. Mc Creary, J. P. and Chao, S. Y., *J. Mar. Res.*, 1985, **43**, 13–36.
8. Bauer, S., Hitchcock, G. L. and Olson, D. B., *Deep Sea Res.*, 1991, **38**, 531–553.
9. Woodruff, S. D., Slutz, R. J., Jenne, R. L. and Steurer, P. M., *Bull. Am. Meteorol. Soc.*, 1987, **68**, 1239–1250.
10. Levitus, S., *Climatological Atlas of the World Ocean. NOAA professional paper no.*13, US Govt Printing Office, Washington DC, 1982, pp. 173.
11. Shetye, S. R., Gouveia, A. D., Shenoi, S. S. C., Sunder, D., Michael, G. S., Almeida, A. M. and Santhanam, K., *J. Mar Res.*, 1990, **48**, 359–378.
12. Muraleedharan, P. M., Ramesh Kumar, M. R. and Gangadhara Rao, L. V., *Continental Shelf Res.*, 1995, **15**, 165–184.

ACKNOWLEDGEMENTS. We thank the Director, National Institute of Oceanography, Goa for providing facilities for the study. This investigation was carried out under the JGOFS programme funded by Department of Ocean Development. This is NIO contribution no. 2504.